

# Infrared-to-visible CW frequency upconversion in Er<sup>3+</sup>-doped fluorindate glasses

Cid B. de Araújo, L. S. Menezes, G. S. Maciel, L. H. Acioli, and A. S. L. Gomes  
*Departamento de Física, Universidade Federal de Pernambuco, 50670-901 Recife PE, Brazil*

Y. Messaddeq,<sup>a)</sup> A. Florez,<sup>b)</sup> and M. A. Aegerter  
*Instituto de Física de São Carlos, Universidade de São Paulo, 13560-970 São Carlos SP, Brazil*

We report on efficient frequency upconversion in Er<sup>3+</sup>-doped fluorindate glasses. The process is observed under 1.48  $\mu\text{m}$  laser diode excitation and results in the generation of strong blue ( $\sim 407$  nm), green ( $\sim 550$  nm), and red ( $\sim 670$  nm) radiation. The main mechanism that allows for upconversion appears to be the energy transfer among Er<sup>3+</sup> ions in excited states. The results illustrate the large potential of this new class of glasses for photonic applications.

Presently there is a great interest in luminescent materials for efficient frequency conversion of infrared radiation into visible light. Among the mechanisms<sup>5</sup> that have been exploited for upconversion, stepwise excited state absorption (ESA) and energy transfer (ET) involving rare earth (RE) ions in a solid may present very large efficiencies.<sup>1-6</sup> These phenomena are useful for detection of infrared radiation by changing this light to the visible range where detectors are more efficient. Also, the operation of upconversion lasers that emit in the blue-green region is another attractive application to obtain short-wavelength sources that can be pumped with diode lasers.

The Er<sup>3+</sup> ion is perhaps the most studied RE ion due to its laser transition, which is also exploited for optical amplification at 1.55  $\mu\text{m}$ .<sup>7</sup> For this application, ESA and ET are deleterious effects that may affect the performance of the amplifier. On the other hand, the studies of upconversion processes in Er<sup>3+</sup>-doped materials are of large interest because Er<sup>3+</sup> exhibits strong fluorescence in the visible and infrared regions, and these transitions can be enhanced by a proper choice of the host material.<sup>8</sup>

Among the new materials available to date, the fluorindate glasses are emerging as a promising group of halide glasses for photonic applications.<sup>9-13</sup> These glasses present high transparency from  $\sim 200$  nm to 8  $\mu\text{m}$ , are resistant to atmospheric moisture, and are capable of incorporating large concentrations of RE ions to the matrix. Recent studies<sup>11-13</sup> have shown their large potential to be used as optical converters, laser hosts, or optical amplifiers, because of the lower multiphonon emission rates and higher fluorescence efficiencies for the doping RE ions than is observed when they are doping other glasses.

In this letter, we report, for the first time to our knowledge, an efficient CW pumped infrared-to-visible upconversion in Er<sup>3+</sup>-doped fluorindate glass. The present study also

offers useful information for the development of visible lasers pumped by infrared laser diodes.

The samples used have the following compositions: (mol %) 39- $x$  InF<sub>3</sub>; 20 ZnF<sub>2</sub>; 16 BaF<sub>2</sub>; 20 SrF<sub>2</sub>; 2 GdF<sub>3</sub>; 2 NaF; 1 GaF<sub>3</sub>;  $x$  ErF<sub>3</sub> ( $x=1,2,3$ ). They were prepared following the procedure given in Ref. 10. Briefly, InF<sub>3</sub> was obtained by fluorination in In<sub>2</sub>O<sub>3</sub> at 400 °C with NH<sub>4</sub>F and HF in a platinum crucible. Then, all fluoride components were mixed and heated in a dry box under argon atmosphere at 700 °C for melting and 800 °C for fining. After this process, the melt was poured and cooled into a preheated brass mold. The samples obtained have good optical quality and volumes of a few cubic centimeters.

The absorption spectra show broad features that can be identified with transitions from the ground state to the excited states of the Er<sup>3+</sup> ion. The positions of the bands and their relative intensities agree with previous reports in other materials.<sup>1-6,8(a)</sup> The spectra obtained for the three samples studied are similar except for the bands intensities and their linewidths, which are dependent on the Er<sup>3+</sup> concentration. The bandwidths of several Angstroms observed are due to the inhomogeneous broadening caused by the crystalline field.

Continuous-wave upconversion fluorescence measurements were performed using a diode laser emitting at 1.48  $\mu\text{m}$  as the excitation source. The sample fluorescence was dispersed by a 0.25 m grating spectrometer and detected by a photomultiplier using either a lock-in or a digital oscilloscope. All measurements were performed at room temperature.

Figure 1 shows the upconversion fluorescence spectrum of one sample under 5.6 mW excitation ( $\sim 170$  W/cm<sup>2</sup>). The observed emissions correspond to transitions in the Er<sup>3+</sup> ions from the excited states to the ground state. The emissions in the visible range correspond to the following transitions:  ${}^2H_{9/2} \rightarrow {}^4I_{15/2}$  ( $\sim 407$  nm);  ${}^2H_{11/2} \rightarrow {}^4I_{15/2}$  ( $\sim 530$  nm);  ${}^4S_{3/2} \rightarrow {}^4I_{15/2}$  ( $\sim 550$  nm); and  ${}^4F_{9/2} \rightarrow {}^4I_{15/2}$  ( $\sim 670$  nm). The lines at  $\sim 550$  and  $\sim 670$  nm are readily visible to the naked eye. Broad spectral features in the region  $\sim 780$  to  $\sim 900$  nm corresponding to  ${}^4I_{9/2} \rightarrow {}^4I_{15/2}$  ( $\sim 808$  nm;

<sup>a)</sup>Present address: Departamento de Química, Universidade do Estado de São Paulo, 14800-900 Araraquara, SP, Brazil.

<sup>b)</sup>On leave from the Departamento de Física, Universidade Industrial de Santander, A.A.678. Bucaramanga, Colombia.

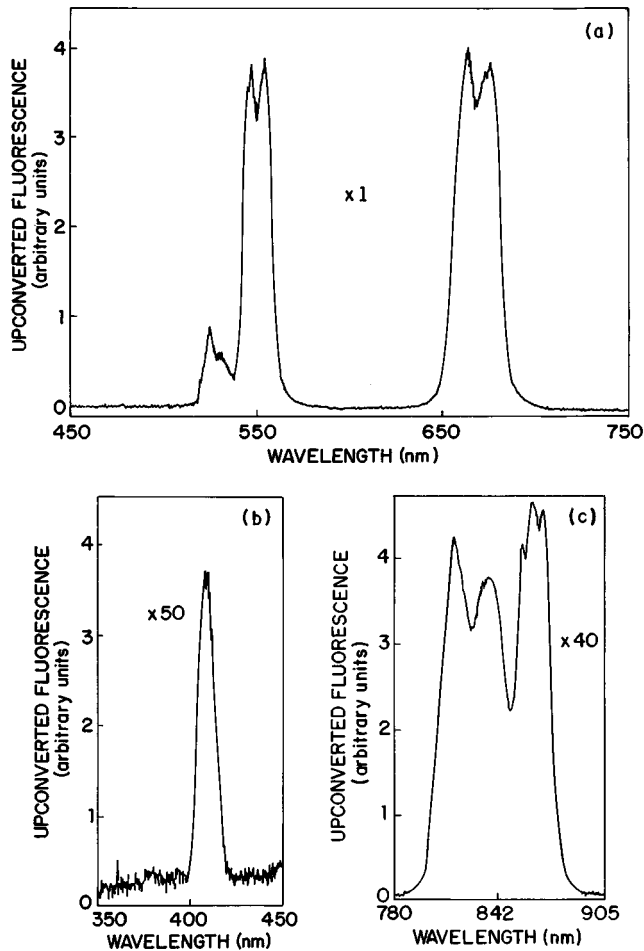


FIG. 1. Upconverted fluorescence in the visible spectrum. The excitation wavelength was  $1.48 \mu\text{m}$  in resonance with the transition  ${}^4I_{15/2} \rightarrow {}^4I_{13/2}$  (sample with  $x=3$ ). The intensities of (b) and (c) have been multiplied by 50 and 40, respectively.

$\sim 827 \text{ nm}$ ) and  ${}^4S_{3/2} \rightarrow {}^4I_{13/2}$  ( $\sim 854 \text{ nm}$ ) were also observed, but their intensities are smaller than the visible transitions.

The spectra were analyzed with respect to their pump power dependence and temporal behavior. To analyze the results, we first note that for any unsaturated upconversion mechanism, the fluorescence signal,  $I_s$ , will be proportional to some power,  $n$ , of the excitation intensity such that  $I_s \propto I^n$ , where  $n=2,3,4,\dots$  is the number of photons absorbed per unconverted photon emitted. In our experiments, the dependence of the fluorescence signal on the excitation intensity was such that  $3.6 < n < 3.9$  for the emission at  $407 \text{ nm}$ ;  $2.4 < n < 2.7$  for the  $550$  and  $670 \text{ nm}$  bands;  $1.7 < n < 2.0$  for the  $808$  and  $872 \text{ nm}$  bands, and  $2.4 < n < 3.3$  for the  $854 \text{ nm}$  emission. The data for one of the samples are shown in Fig. 2. From the intensity dependence observed and the wavelength of the emitted radiations, we conclude that four laser photons are involved in the  $1.48 \mu\text{m}$  to  $407 \text{ nm}$  conversion, three laser photons participate in the  $1.48 \mu\text{m}$  to  $550 \text{ nm}$ ,  $1.48 \mu\text{m}$  to  $670 \text{ nm}$ , and  $1.48 \mu\text{m}$  to  $854 \text{ nm}$  conversions, and two incident photons produce the  $1.48 \mu\text{m}$ -to- $808 \text{ nm}$  and  $1.48 \mu\text{m}$  to  $827 \text{ nm}$  upconversions. The deviations from the exact  $n$  values are due to the strong absorption at  $1.48 \mu\text{m}$  and the absorption of the unconverted fluorescence, and

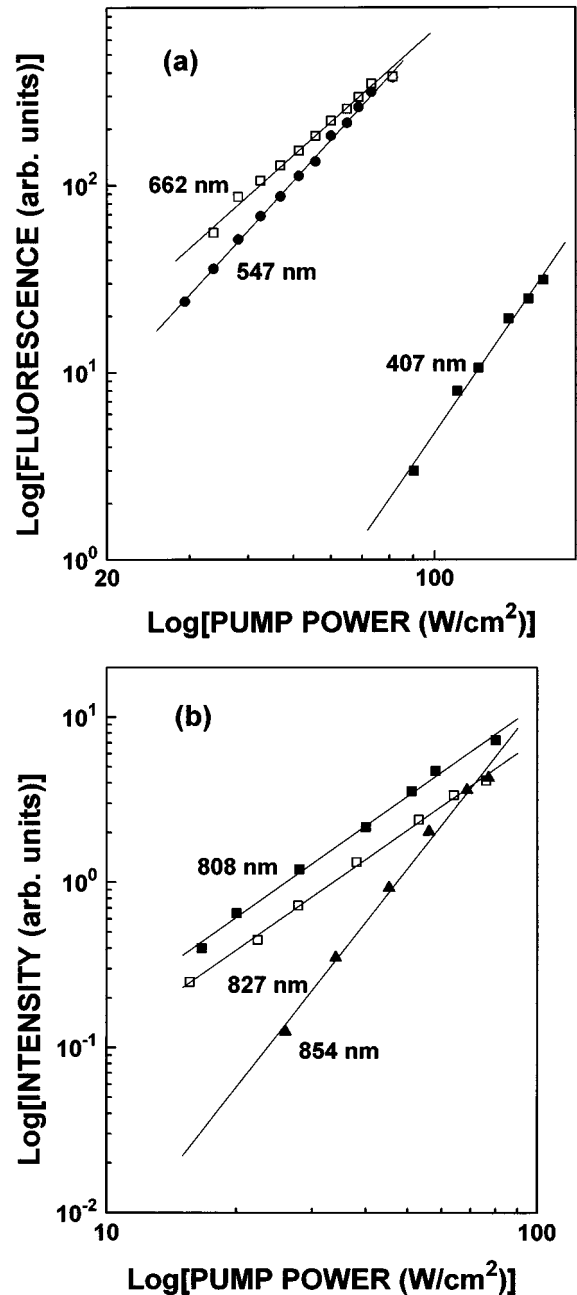


FIG. 2. Fluorescence output intensity as a function of the input laser intensity (sample with  $x=2$ ). Straight lines with different slopes  $n$  are obtained for each wavelength: (a)  $n=3.6$  ( $407 \text{ nm}$ );  $n=2.7$  ( $547 \text{ nm}$ );  $n=2.4$  ( $662 \text{ nm}$ ); (b)  $n=1.8$  ( $808 \text{ nm}$ ),  $n=1.8$  ( $827 \text{ nm}$ ), and  $n=3.3$  ( $854 \text{ nm}$ ).

because the non-radiative decay from higher lying states to the fluorescent states may also contribute to the intensities of the observed spectral lines.

Figure 3 shows the relevant  $\text{Er}^{3+}$  energy levels together with two possible upconversion processes and the observed fluorescence lines.

Different processes may lead to the population of highly excited  $\text{Er}^{3+}$  states after excitation in the near infrared.<sup>1-6</sup> These processes rely either on multistep ESA or ET between  $\text{Er}^{3+}$  neighbors. The ET process in which an excited ion nonradiatively transfers its energy to an already excited neighbor is one of the most efficient mechanisms, and has

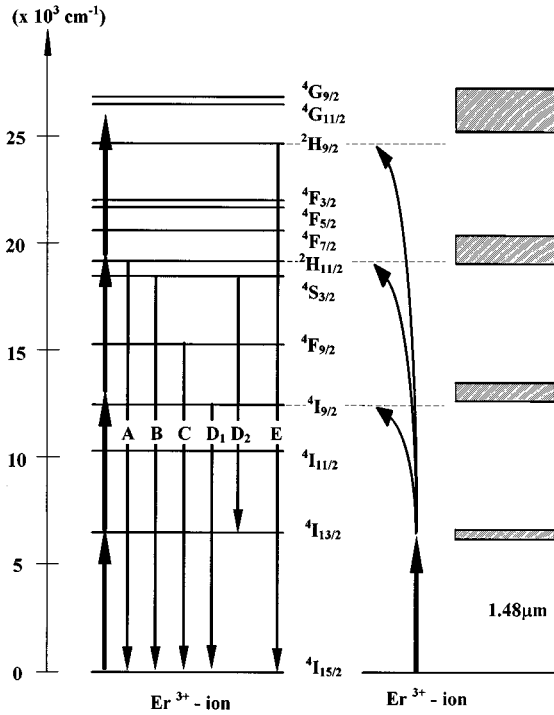


FIG. 3. Simplified energy levels scheme for  $\text{Er}^{3+}$  in the fluoroindate glass. The downward arrows indicate the observed upconverted fluorescence and the curved arrows on the right side represent energy transfer. The letters beside the straight arrows correspond to the following spectral lines: A ( $\sim 530$  nm); B ( $\sim 550$  nm); C ( $\sim 670$  nm);  $D_1$  ( $\sim 808$  and  $\sim 827$  nm);  $D_2$  ( $\sim 854$  nm); and E ( $\sim 407$  nm).

been observed in a larger number of systems including fluoroindate glasses.<sup>12,13</sup> This mechanism can arise from electric multipole or exchange interactions, and its rate constant depends on the ion-ion separation. Here, we expect that ET is the dominant process because of the large  $\text{Er}^{3+}$  concentration in our samples, and because the intermediate ESA step ( ${}^4I_{13/2} \rightarrow {}^2H_{11/2}$ ) is a two-photon transition with small probability to occur due to the weak laser intensity used. Therefore, the most relevant pathway for upconversion initiates with the transition  ${}^4I_{15/2} \rightarrow {}^4I_{13/2}$ . Afterwards, ET between two excited  $\text{Er}^{3+}$  ions at the  ${}^4I_{13/2}$  level will take one ion to the  ${}^4I_{9/2}$  level. This step is followed by two other successive transfer processes from ions at the  ${}^4I_{13/2}$  state, which result in the excitation to the higher levels  ${}^4G_{9/2}$ ,  ${}^4G_{11/2}$ , and  ${}^3H_{9/2}$ . After nonradiative decay to the states  ${}^2H_{11/2}$ ,  ${}^4S_{3/2}$ ,  ${}^4F_{9/2}$ , and  ${}^4I_{9/2}$ , radiative transitions to the ground state give rise to the observed upconverted visible fluorescence. The infrared emissions are due to transitions  ${}^4I_{9/2} \rightarrow {}^4I_{15/2}$  and  ${}^4S_{3/2} \rightarrow {}^4I_{13/2}$ .

To characterize the temporal evolution of the signals, another series of experiments was performed. The laser beam was chopped at 8 Hz and the fluorescence was observed with a time resolution better than 1 ms. The signal corresponding to the various upconverted emissions grew to their maximum value in  $\tau_r < 15$  ms and decay in  $\tau_d < 6$  ms. In general, the rise and decay times decrease for increasing concentrations, and for the range of  $\text{Er}^{3+}$  concentrations studied,  $\tau_d$  and  $\tau_r$  change up to  $\sim 50\%$ .

In order to understand the observed behavior, we first recall that the efficiency of upconversion depends on the probability of ESA or ET between adjacent excited ions, as well as the quantum efficiency of the emitting level. By either process, the dynamics of the upconversion signals depends on the lifetime of the intermediate excited states involved. For the samples used, the lifetime of the states  ${}^2H_{9/2}$ ,  ${}^4S_{3/2}$ ,  ${}^4F_{9/2}$ , and  ${}^4I_{11/2}$  were reported in Ref. 12. The values obtained for the same range of  $\text{Er}^{3+}$  concentrations were  $\tau({}^2H_{9/2}) \sim 15\text{--}20$   $\mu\text{s}$ ,  $\tau({}^4S_{3/2}) = 86\text{--}573$   $\mu\text{s}$ ,  $\tau({}^4F_{9/2}) = 302\text{--}645$   $\mu\text{s}$ , and  $\tau({}^4I_{11/2}) = 10.6\text{--}9.4$  ms. The lifetimes of the states  ${}^4I_{9/2}$  and  ${}^4I_{13/2}$  were not measured, but on the basis of the results for other host materials,<sup>1-6,8(a)</sup> we expect that they are of the same order of magnitude as  $\tau({}^4I_{11/2})$ . Such long lifetimes are determined by the multiphonon relaxation rates, which are small because of the small phonon energies associated with the fluoroindate matrix. Thus, considering that the states  ${}^4I_{9/2}$  and  ${}^4I_{13/2}$  are likely to participate in the upconversion processes, we conclude that the long values observed for  $\tau_r$  and  $\tau_d$ , provide a favorable evidence for the relevance of the ET mechanism.

Although ESA may also contribute for the generation of the upconverted radiation, its contribution is expected to be very small in the present case. For samples with smaller  $\text{Er}^{3+}$  concentration, both processes may become equally relevant, and the selection of the proper  $\text{Er}^{3+}$  concentration is an important step for each kind of application.

This work was supported by the Brazilian Agencies Conselho Nacional de Desenvolvimento Científico e Tecnológico (CNPq), Financiadora Nacional de Estudos e Projetos (FINEP), and Fundação de Apoio à Pesquisa (FACEPE). We also thank Blenio J. P. da Silva for polishing the samples and TELEBRÁS for the loan of the diode laser used.

- <sup>1</sup> B. R. Reddy and P. Venkateswarlu, Appl. Phys. Lett. **64**, 1327 (1994).
- <sup>2</sup> M. Shojiya, M. Takahashi, R. Kanno, Y. Kawamoto, and K. Kadono, Appl. Phys. Lett. **65**, 1874 (1994).
- <sup>3</sup> M. P. Hehlen, G. Frei, and H. U. Güdel, Phys. Rev. B **50**, 16264 (1994); A. Gharavi and G. L. McPherson, Appl. Phys. Lett. **61**, 2635 (1992).
- <sup>4</sup> A. S. L. Gomes, C. B. de Araújo, B. J. Ainslie, and S. P. Craig-Ryan, Appl. Phys. Lett. **57**, 2169 (1990).
- <sup>5</sup> S. Tanabe, S. Yoshi, K. Hirao, and N. Soga, Phys. Rev. B **45**, 4620 (1992).
- <sup>6</sup> P. Xie and S. C. Rand, Appl. Phys. Lett. **63**, 3125 (1993).
- <sup>7</sup> E. Desurvire and J. R. Simpson, J. Lightwave Technol. **7**, 835 (1989).
- <sup>8</sup> (a) X. Zou and T. Izumitani, J. Non-Cryst. Solids **162**, 68 (1993) and references therein; (b) F. E. Auzel, Proc. IEEE **61**, 758 (1973).
- <sup>9</sup> T. Sugana, Y. Miyasima, and T. Komuki, Electron. Lett. **26**, 2042 (1990); K. Annapura, M. Hanumanthu, and S. Buddhudu, Spectrochim. Acta **48A**, 791 (1992); J. Fernandez, R. Bolda, and M. A. Arriandiago, Opt. Mater. **4**, 91 (1994).
- <sup>10</sup> Y. Messaddeq and M. Poulain, Mater. Sci. Forum **67/68**, 161 (1991).
- <sup>11</sup> R. M. Almeida, J. C. Pereira, Y. Messaddeq, and M. A. Aegerter, J. Non-Cryst. Solids **161**, 105 (1993).
- <sup>12</sup> R. Reiche, L. A. O. Nunes, C. C. Carvalho, Y. Messaddeq, and M. A. Aegerter, Solid State Commun. **85**, 773 (1993).
- <sup>13</sup> L. E. E. de Araújo, A. S. L. Gomes, Cid B. de Araújo, Y. Messaddeq, A. Florez, and M. A. Aegerter, Phys. Rev. B **50**, 16219 (1994).